J Mater Sci (2006) 41:7387–7392
DOI 10.1007/s10853-006-0811-3

Microstructure evolution in adiabatic shear band in α-titanium

Y. Yang · B. F. Wang

Received: 5 September 2005 / Accepted: 5 December 2005 / Published online: 20 September 2006

Abstract The microstructure and microtexture of adiabatic shear bands (ASBs) on the titanium side of a titanium/mild steel explosive cladding interface are investigated by means of optical microscopy (OM), scanning electron microscopy/electron back-scattered diffraction (SEM/EBSD) and transmission electron microscopy (TEM). Highly elongated subgrains and fine equiaxed grains with low dislocation density are observed in the ASBs. Recrystallization microtextures (28°, 54°, 0°), (60°, 90°, 0°) and (28°, 34°, 30°) are formed within ASBs. The grain boundaries within ASBs are geometrical necessary boundaries (GNBs) with high-angles. Based on the relations between temperature and the engineering shear strain, the temperature in the ASBs is estimated to be about 776–1142 K (0.4–0.6 T_m). The rotation dynamic recrystallization (RDR) mechanism is employed to describe the kinetics of the nano-grains' formation and the recrystallized process within ASBs. The small grains within ASBs are formed during the deformation and do not undergo significant growth by grain boundary migration after deformation.

Introduction

Adiabatic shear banding is an important thermoviscoplastic instability mode of materials at high strain rates. Due to the properties of low heat conductivity and high adiabatic shearing sensitivity, adiabatic shear bands (ASBs) are easily observed in titanium and its alloys. Meyers et al. [1], Yang et al. [2], and Chichili et al. [3] investigated the microstructure in ASBs of commercial pure titanium by means of optical microscopy (OM), scanning electron microscopy (SEM) and transmission electron microscopy (TEM), and suggested that the structure was formed by the dynamic recrystallization. However, Pérez-Prado et al. [4] observed the microstructure in ASBs of Ta and Ta–W alloys and proposed that dynamic recrystallization was not occurring in ASBs. Ring-like electron diffraction patterns were also observed in severely deformed fine grains formed by dynamic recovery [4]. Electron Back-Scattered Diffraction (EBSD) can readily obtain the crystallographic orientation of grains and characteristics of grain boundaries. This method combined with TEM is helpful to elucidate the microstructure in ASBs of pure titanium and the deformation/recrystallization mechanism.

The objectives of this paper are to report observations of the microstructure and microtexture in ASBs on the titanium side of a titanium/mild steel explosive cladding interface and to discuss the microstructure evolution in ASBs.

Experimental

Commercially pure titanium [TA2(α-Ti)] and mild steel (A3) are used in the present work. The α-Ti/A3 composite plate was formed by the constant stand-off explosive cladding technique [2]. The impact velocity is 608 m/s. The pressure corresponding to this

Y. Yang (✉) · B. F. Wang
School of Materials Science and Engineering, Central South University, Changsha 410083 Hunan, People's Republic of China
e-mail: yangyang@mail.csu.edu.cn

velocity is approximately 8400 MPa, the strain rate is 5×10^5–10^6 s^{-1} and the shear strain is about 5. The deformation time (t) is simply given by the total strain divided by the strain rate, that is 5–10 μs. Specimens for analyses were cut from the central portion of the sheets in a plane parallel to the jetting direction and normal to the plane of the cladding interface. The chemical attack for TA2 is 4 ml HNO_3+6 ml HCl+5 ml HF+100 ml H_2O; the A3 side is not attacked. Investigations of OM were performed with a POLYVAR-MET microscope. TEM observations were carried out with a JEOL-2010 transmission electron microscope operated at 200 kV. The orientation imaging microscopy (OIM) was carried out with a Hitachi-S4300 FE SEM integrated with a computer aided EBSD system from TSL OIM 2.6 operated at 20 kV. Due to the spatial resolution of the EBSD technique (~0.2 μm), orientation data could only be acquired in isolated locations in ASBs. For convenience, two sections of $\phi_2 = 0°$, 30° in the orientation distribution function (ODF) are used to illustrate texture components.

Results and discussion

Microstructures

Figure 1 shows an optical micrograph of a TA2/A3 explosive cladding interface. ASBs on the TA2 side are parallel to each other and have an approximately 45° inclination to the interface plane. No ASBs are observed on the mild steel side because of differences in physical, mechanical, thermal properties and crystal structure [2].

Figure 2a shows the transition region between the ASBs and the matrix. Close to the boundary of the shear band, highly elongated subgrains, approximately 0.1 μm in width, with thick cell walls are observed. Dislocation tangling and thick cell wall formation suggest that dislocations are active and consistent with high strain levels in the boundary. Figure 2b shows equiaxed grains in the center of an ASB. The sizes of equiaxed grains with low dislocation density are about 0.05–0.2 μm in diameter. The characteristics of grains are obviously different from the grains in the boundary of shear band and the matrix. The ring-like selected area diffraction (SAD) pattern inserted in Fig. 2b can be indexed as close-packed hexagonal (HCP) structure of α-Ti. It indicates that a large number of small grains with high angle grain boundaries are present in the center of the ASB and the α-Ti (HCP) → β-Ti (BCC) transformation does not occur. These features are similar to those observed in recrystallization.

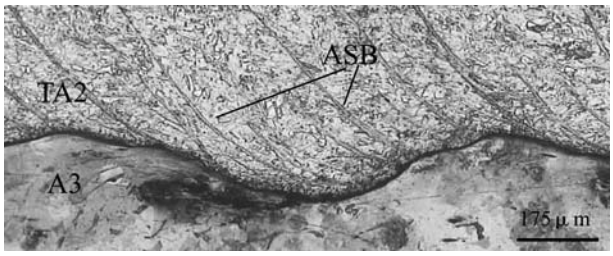

Fig. 1 Optical micrograph of the titanium/mild steel explosive cladding interface

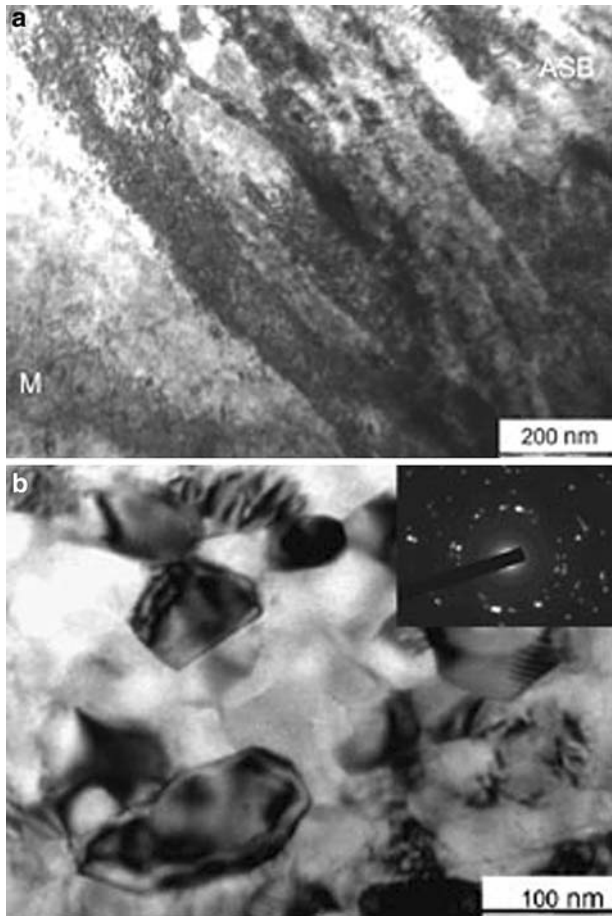

Fig. 2 Transmission electron micrograph of ASB: (**a**) bright-field image of the transition region of the shear band and matrix, and (**b**) bright-field image of equiaxed fine grains in the core of shear band and the corresponding diffraction pattern

Microtexture measurement

The EBSD technique was used to measure the local orientations of grains within the ASBs and in a region adjacent to them. From the measured orientations, the

ODFs are calculated and shown in Fig. 3. The ϕ_1, ϕ and ϕ_2 angles are the conventional Euler angles. The orientation data are rotated and then the reference system is taken so that the shear plane normal (SPN) and the shear direction (SD) are parallel to *x*- and *y*-axes of the figure, shown in Fig. 3a.

Figure 3 illustrates microtextures of grains within an ASB and in a region adjacent to it. It can be seen that grains adjacent to the shear band are elongated in the shear direction. Grains adjacent to and in the core of the ASB can be chosen by the OIM analysis software and the ODF can also be obtained as shown in Fig. 3b and c, respectively. Figure 3c shows that a fiber texture is formed in the core of shear band and it is similar to that obtained in the grains adjacent to shear band, shown in Fig. 3b. The point-to-point misorientations are plotted versus distance along path A, as shown in Fig. 3d. It can be seen that misorientation between the grains in the ASB is much larger than 15°. Liu and Hansen [5] had classified deformation-induced boundaries into incidental dislocation boundaries (IDBs) and geometrical necessary boundaries (GNBs). The cellblock structures were bounded by GNBs and the ordinary dislocation cell structures were bounded by IDBs. The misorientation across GNBs should be much larger than across IDBs and should rise faster with increasing strain [5]. In order to accommodate the imposed shear strain and maintain neighboring grains compatibility, grains in ASBs continue to subdivide and the resulting grain boundaries are high-angle GNBs.

Besides the fiber texture described the above, the microtextures of grains in the core of ASBs are peaked at (28°, 54°, 0°), (60°, 90°, 0°) and (28°, 34°, 30°), shown in Fig. 3c. These microtextures are obviously different to those deformation textures in neighboring regions. Therefore, recrystallization should be occurring in the ASBs.

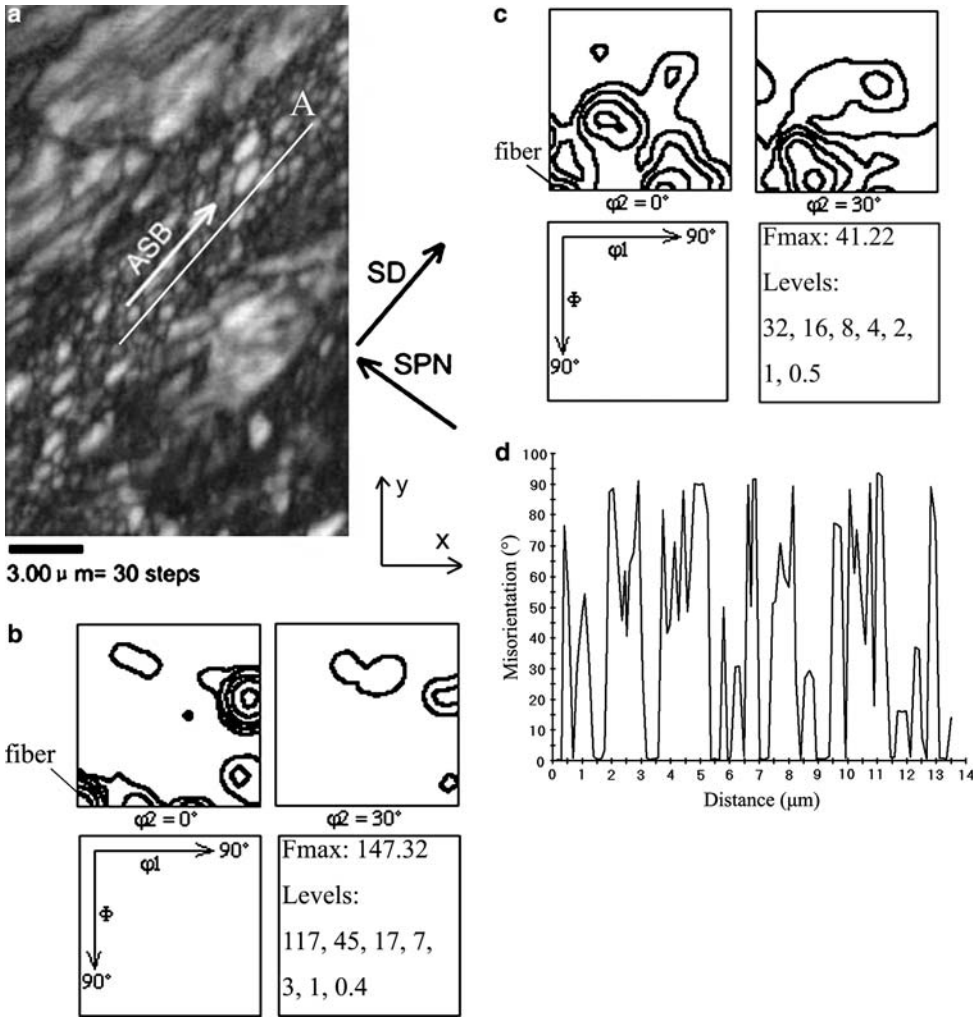

Fig. 3 (**a**) OIM map showed grains within and adjacent to the shear band. (**b**) ODF of the grains adjacent to the shear band. (**c**) ODF of the grains within shear band. (**d**) Point to point misorientation along path in (**a**)

Estimate of temperature within Adiabatic Shear Bands

At high strain rates ($> 10^3$ s^{-1}), the adiabatic temperature rise in ASBs is calculated by the following equation [2, 6].

$$T - T_0 = \frac{0.9}{\rho c}\int_0^{\varepsilon} \sigma d\varepsilon \tag{1}$$

where T is the temperature within the ASBs, T_0 is the environmental temperature, ρ is mass density, c is heat capacity, ε is plastic strain and σ is stress calculated by a constitutive equation.

The α-Ti is a highly rate sensitive material. The constitutive response of it can be described as the Zerilli–Armstrong equation [7]:

$$\sigma = \sigma_0 + B\mathrm{e}^{-(\beta_0-\beta_1 \ln \dot{\varepsilon})T} + B_0\varepsilon^{C_n}\mathrm{e}^{-(\alpha_0-\alpha_1 \ln \dot{\varepsilon})T} \tag{2}$$

Where σ_0, B, B_0, C_n, α_0, α_1, β_0 and β_1 are the parameters determined by a regression analysis procedure. Their values for α-Ti obtained by Xue et al. [7] are 0 MPa, 990 MPa, 1.1×10^{-4} K^{-1}, 7.5×10^{-5} K^{-1}, 0.5, 700 MPa, 2.24×10^{-3} K^{-1} and 9.73×10^{-5} K^{-1}, respectively. The data set includes high rate data up to 2.5×10^5 s^{-1}.

The heat capacity of α-Ti is given by

$$C(T) = 0.514 + 1.357 \times 10^{-4}T - 3.366 \times 10^3 T^{-2} + 2.767 \times 10^{-8}T^2 [\mathrm{J/kg\,K}] \tag{3}$$

Substituted Eq. (3) into Eq. (1) and combined with Eq. (2), the relation between temperature and true strain is obtained. Culver [8] introduced a simple relation between true strain and engineering shear strain.

$$\gamma = \sqrt{2\mathrm{e}^{2\varepsilon} - 1} - 1 \tag{4}$$

It should be mentioned that this conversion relation is for simple shear case. The state of stress for the formation of ASBs under explosive clad loading is of approximate pure shears. From Eqs. (1–4), the relations between temperature and the engineering shear strain are plotted in Fig. 4. The shear band temperature is expressed as a function of engineering shear strain at different strain rates. In order to conveniently express the relationship between temperature and shear strain, a polynomial function is used to fit the curve when the strain rate is 5×10^5 s^{-1}. The result shows that the following function fits the original data well, as shown in Fig. 4.

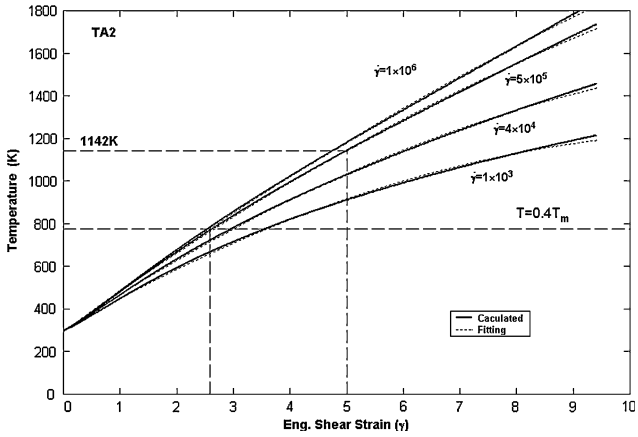

Fig. 4 Calculations predict temperature rise within shear band in titanium at different strain rates

$$T = -4.3985\gamma^2 + 192.5605\gamma + 293.1518 \tag{5}$$

In the present works, the strain rate is approximately 5×10^5–10^6 s^{-1} and the deformation time is 5–10 μs. When the strain rate reaches 5×10^5 s^{-1}, the temperature within the ASBs is 0.4 T_m (776 K) at a strain $\gamma = 2.58$ (the corresponding time ≈ 5 μs), as shown in Fig. 4. The maximum adiabatic temperature is determined to be 1142 K when the deformation have ceased (the corresponding time ≈ 10 μ s), as shown in Fig. 4. It can be concluded that the adiabatic temperature in the ASBs should be 776–1142 K (0.4–0.6 T_m).

Recrystallization mechanism

The formation of ASBs includes the deformation and the cooling processing. The above analysis of the microstructure and microtexture of the ASBs suggest that the rotational dynamic recrystallization (RDR) mechanism took effect on the microstructure evolution.

According to RDR, the process of subgrain boundaries rotating to form high angle boundaries is driven by the minimization of the interfacial energy, and is described as following equation [6]:

$$t = \frac{L_1 kTf(\theta)}{4\delta\eta D_{b0}\exp(-Q_b/RT)} \tag{6}$$

where t is time, δ is grain-boundary thickness, η is the grain boundary energy, D_b0 is a constant related to grain boundary diffusion, L_1 is the average subgrain diameter, Q_b is the activation energy for grain boundary diffusion, θ is the subgrain misorientation. Here $Q_b = (0.4 - 0.6)Q$ is chosen and Q is the activation energy for grain growth, and

$$f(\theta) = \frac{3\tan(\theta) - 2\cos(\theta)}{3 - 6\sin(\theta)} + \frac{2}{3} - \frac{4\sqrt{3}}{9}\ln\frac{2+\sqrt{3}}{2-\sqrt{3}} + \frac{4\sqrt{3}}{9}\ln\frac{\tan(\theta/2) - 2 - \sqrt{3}}{\tan(\theta/2) - 2 + \sqrt{3}} \quad (7)$$

The parameters for commercially pure titanium used in Eq. (6) are $\delta = 6.0 \times 10^{-10}$ m, $\eta = 1.19$ J m^{-2}, $D_b0 = 1.0 \times 10^{-5}$ m^{2}s^{-1}, $Q = 204$ kJ mol^{-1}, $k = 1.38 \times 10^{-23}$ J K^{-1}, $R = 8.314$ J mol^{-1} [9]. According to the RDR mechanism, the subgrains need to rotate about 30 ° to form recrystallized grains. Therefore, from Eq. (7), some predictions are obtained. In Fig. 5a, the temperature is varied from 0.35 to 0.5 T_m for a subgrain size of 100 nm; in Fig. 5b, the subgrain size L_1 is varied from 100 nm to 1 μm at T=0.45 T_m (873 K).

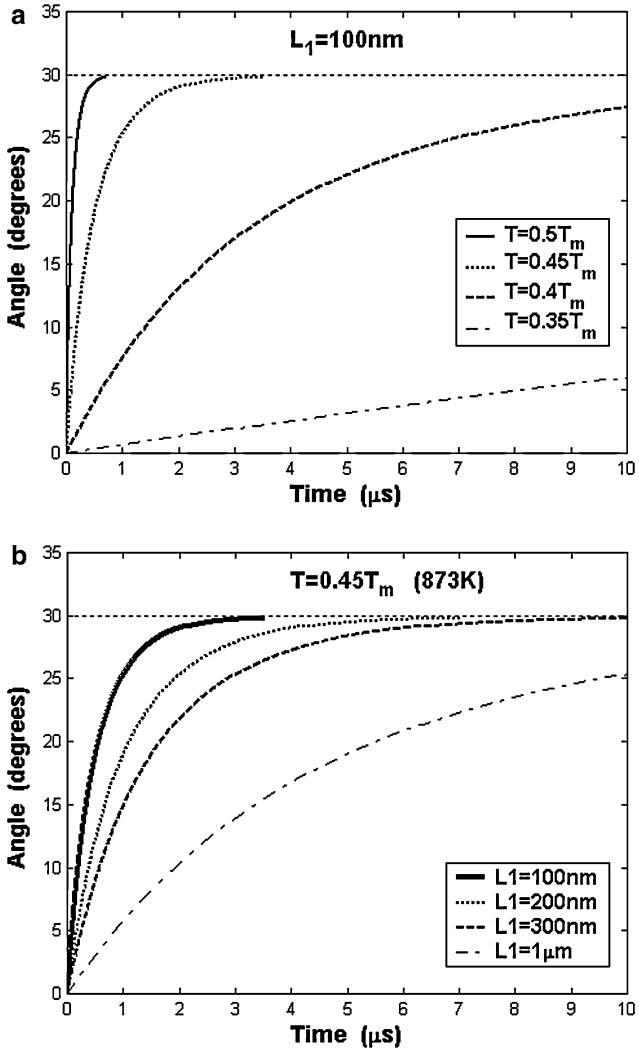

Fig. 5 Angle of rotation of subgrain boundary in titanium as a function of need time for (**a**) different temperatures for L_1 = 100 nm and (**b**) different subgrain size at 0.45 T_m

Larger subgrain size and lower temperature result in more time needed for recrystallization.

Substituting Eq. (5) into Eq. (6), the angle of subgrain rotation as a function of time for subgrain size L_1 = 100 nm is obtained as shown in Fig. 6. The rotation angle θ is very small in the region [A → B] since during the early stage of deformation, dislocations in the severe deformation zone are accumulated to form elongated cell structures and those cell structures break up to form subgrains. The subgrain misorientation reaches 5° at about 4.5 μs corresponding to $\gamma = 2.25$ and T is 700 K. The subgrain rotation asymptotically approaches 30° within about 2 μs in the region [C → D]. To RDR mechanism, the subgrains rotating sharply suggest that dynamic recrystallization begun. The critical recrystallization temperature is 700 K, which is lower than the conventional recrystallization beginning temperature (0.4 T_m, 776 K) because the high dislocation density increases the driving force for recrystallization. The needed time for subgrains with diameters of 100 nm rotate to high angle boundaries (> 15°) is less than 3 μs, as shown in Fig. 5b. The total deformation time is 5–10 μs. Thus, fine equiaxed grains with diameters smaller or equal to 100 nm can be formed during the deformation processing.

During the cooling stage, the RDR cannot be took effect due to the absence of mechanical assistance, and the microstructure evolution must to be a migrational mechanism. Migrational recrystallization mechanisms are based on diffusion, which is temperature dependent and is surely occur when the temperature becomes very high. According to migrational recrystallization mechanisms, the recrystallized grain

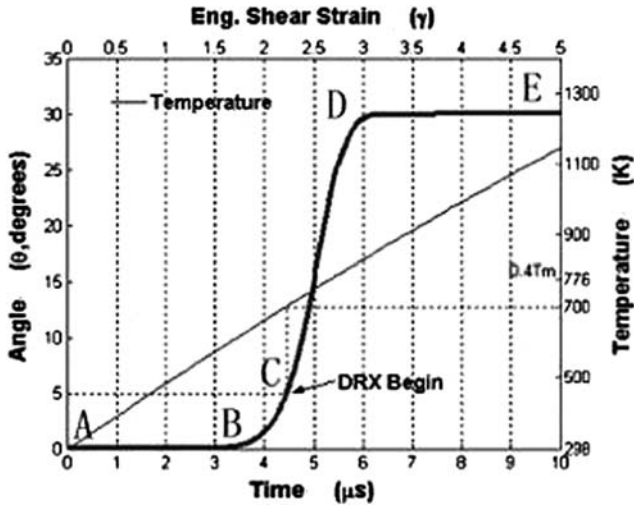

Fig. 6 Angle of subgrain rotation in titanium as a function of time for subgrain size L_1 = 100 nm

size is calculated by the following grain growth equation [10].

$$d \cong k_0 \sum_{i=0}^{N} \left[\exp\left(-\frac{Q}{2RT(t_i)} \right) \right] \Delta t^{1/n} \quad (8)$$

where k_0, n are material constants, and Δt is the change in time. For pure Ti, k_0 and n are equal to 4.3 and 1, respectively [10]. During the whole process including the deformation and the cooling, the calculated grain size d is about 0.12 nm, which is much smaller than the observed 50 nm. So, it is concluded that migrational recrystallization mechanisms are too slow to account for the observed recrystallized microstructures.

Therefore, the observed recrystallized nano-grains are formed during the deformation. If the new recrystallized grains are formed by the RDR mechanism, they have not undergone significant growth by grain boundary migration.

Conclusion

The microstructures in ASBs in α-Ti are fine equiaxed grains with low dislocation density, approximately 0.05–0.2 μm in diameter in the core, and highly elongated subgrains with thick cell walls in the boundary of the shear band. Recrystallization microtextures (28°, 54°, 0°), (60°, 90°, 0°) and (28°, 34°, 30°) are formed in the ASBs. The grain boundaries in ASBs are GNBs with high-angle. Based on the relations between temperature and the engineering shear strain, the temperature within the ASBs is estimated to be about 776–1142 K. The kinetics of formation of the fine grains is successful calculated by the RDR mechanism. The small grains within ASBs are formed during the deformation and do not undergo significant growth by grain boundary migration after deformation. Within the deformation time (5–10 μs), the grains can carry out the following process: Dislocations accumulate to form elongated cell structures, cell structures break up to form subgrains, subgrains rotate and finally form recrystallized grains.

Acknowledgements This work is supported by the Ph. D. Programs Foundation of Ministry of Education of China, No. 20020533015 and by National Nature Science Foundation of China, No. 50471059.

References

1. Meyers MA, Pak HR (1986) Acta Metall 34:2493
2. Yang Y, Zhang XM, Li ZH (1996) Acta Mater 44:561
3. Chichili DR, Ramesh KT, Hemker KJ (2004) J Mech Phys Solids 52:1889
4. Pérez-Prado MT, Hines JA, Vecchio KS (2001) Acta Mater 49:2905
5. Liu Q, Hansen N (1995) Scripta Metall Mater 32:1289
6. Meyers MA, Xu YB, Xue Q et al. (2003) Acta Mater 51:1307
7. Xue Q, Meyers MA, Nesterenko VF (2002) Acta Mater 50:575
8. Culver RS (1973) In: Rohde RW, Butcher BM, Holland JR (eds) Metallurgical effects at high strain rates. Plenum Press, New York, p 519
9. Yong QL, Tian JG (1999) J Yunnan Polytechnic Univ 15:7
10. Meyers MA, Nesterenko VF et al (2001) Mater Sci Eng A A317:204